

Bayesian analysis of radial velocity data of GJ667C with correlated noise: evidence for only 2 planets

F. Feroz^{*} and M. P. Hobson

Astrophysics Group, Cavendish Laboratory, JJ Thomson Avenue, Cambridge CB3 0HE, UK

Accepted —. Received —; in original form 27 February 2024

ABSTRACT

GJ667C is the least massive component of a triple star system which lies at a distance of about 6.8 pc (22.1 light-years) from Earth. GJ667C has received much attention recently due to the claims that it hosts up to seven planets including three super-Earths inside the habitable zone. We present a Bayesian technique for the analysis of radial velocity (RV) data-sets in the presence of correlated noise component (“red noise”), with unknown parameters. We also introduce hyper-parameters in our model in order to deal statistically with under or over-estimated error bars on measured RVs as well as inconsistencies between different data-sets. By applying this method to the RV data-set of GJ667C, we show that this data-set contains a significant correlated (red) noise component with correlation timescale for HARPS data of order 9 days. Our analysis shows that the data only provides strong evidence for the presence of two planets: GJ667Cb and c with periods 7.19d and 28.13d respectively, with some hints towards the presence of a third signal with period 91d. The planetary nature of this third signal is not clear and additional RV observations are required for its confirmation. Previous claims of the detection of additional planets in this system are due the erroneous assumption of white noise. Using the standard white noise assumption, our method leads to the detection of up to five signals in this system. We also find that with the red noise model, the measurement uncertainties from HARPS for this system are under-estimated at the level of ~ 50 per cent.

Key words: stars: planetary systems – stars: individual: GJ667C – techniques: radial velocities – methods: data analysis – methods: statistical

1 INTRODUCTION

Extrasolar planetary research has made great advances in the last decade as a result of the data gathered by several ground and space based telescopes and thus far more than 900 extrasolar planets have been discovered. More and more planets with large orbital periods and small velocity amplitudes are now being detected due to remarkable improvements in the accuracy of RV measurements. With the flood of new data, more powerful statistical techniques are being developed and applied to extract as much information as possible. Traditionally, the orbital parameters of the planets and their uncertainties have been obtained by a two stage process. First the period of the planets is determined by searching for periodicity in the RV data using the Lomb–Scargle periodogram (Lomb 1976; Scargle 1982). Other orbital parameters are then determined using minimisation algorithms, with the orbital period of the planets fixed to the values determined by Lomb–Scargle periodogram.

Bayesian methods have several advantages over traditional methods, for example when the data do not cover a complete orbital phase of the planet. Bayesian inference also provides a rig-

orous way of performing model selection which is required to decide the number of planets favoured by the data. The main problem in applying such Bayesian model selection techniques is the computational cost involved in calculating the Bayesian evidence. Nonetheless, Bayesian model selection has the potential to improve the interpretation of existing observational data and possibly detect yet undiscovered planets. Recent advances in Marko-Chain Monte Carlo (MCMC) techniques (see e.g. Mackay 2003) have made it possible for Bayesian techniques to be applied to extrasolar planetary searches (see e.g. Gregory 2005; Ford 2005; Ford & Gregory 2007; Balan & Lahav 2009). Feroz, Balan & Hobson (2011) presented a new Bayesian method for determining the number of extrasolar planets, as well as for inferring their orbital parameters, without having to calculate directly the Bayesian evidence for models containing a large number of planets.

GJ667 is an M dwarf in a triple star system which lies at a distance of about 6.8 pc (22.1 lightyears) from Earth. GJ667C is the least massive component of this system with mass $0.33 \pm 0.03 M_{\odot}$ (Delfosse et al. 2013). Two other components of this system, GJ667AB, are a closer couple of K dwarfs with semi-major axis of 1.82 AU, period of 42.15 years and mass of $1.27 M_{\odot}$ (Söderhjelm 1999). GJ667C is at a projected distance of

^{*} E-mail: f.feroz@mrao.cam.ac.uk

32.4'' from GJ667AB, giving an expected semi-major axis of ~ 300 AU (Delfosse et al. 2013). Using the data from the HARPS spectrograph (with RVs obtained using cross-correlation function ‘CCF’ technique), Bonfils et al. (2011) reported detection of a planet (GJ667Cb) with orbital period of 7.2d and minimum mass of $5.9M_{\oplus}$. They also found evidence for the presence two further planets with orbital periods 28d and 90d respectively. 7.2d and 28d planets were confirmed by Anglada-Escude et al. (2012) and Delfosse et al. (2013), both using HARPS data although reduced using different techniques. GJ667Cc with orbital period of 28d is particularly interesting as it lies well within the habitable zone of the host star where it could support liquid water. Anglada-Escude et al. (2012) further found evidence for one additional planet with orbital period 75d, however they did not consider it significant since it was affected by aliasing interactions with another 91d signal and the likely rotation period of the star at 105 days. Delfosse et al. (2013) found a signal with orbital period 106d but attributed it to the stellar rotation due to it being very close to the rotation period of the star. A Bayesian analysis of the HARPS RVs for this system was performed by Gregory (2012), who apart from confirming the presence of first two planets GJ667Cb and c, also found evidence for four additional signals with orbital periods 30.82d, 38.82d, 53.22d and 91.3d respectively. They discarded the 53.22d signal due to the high likelihood of it being the second harmonic of the stellar rotational period. Potential planets with 30.82d and 38.82d orbital periods lie in the central region of their host star’s habitable zone and therefore are of much interest.

More recently, Anglada-Escude et al. (2013) performed a joint analysis of RV observations of this system from HARPS, HIRES/Keck and PFS/Magellan spectrographs (available from Anglada-Escude & Butler 2012). Instead of using the CCF technique to obtain RVs from observed spectra, they used the Template-Enhanced Radial velocity Re-analysis Application ‘TERRA’ technique which has been claimed to produce significantly more accurate RVs compared to RVs obtained using the CCF technique (Anglada-Escude & Butler 2012). Anglada-Escude et al. (2013) found evidence for the existence of six (even seven) planets GJ667Ca-f with period 7.2d, 28d, 92d, 62d, 39d and 260d (seventh one having period of 17d) respectively. They further showed that this system is dynamically stable. All these planet candidates have relatively low masses (\sim few M_{\oplus}) with GJ667Cc, e and f lying inside the habitable zone, which if confirmed, would make GJ667C one of the first systems with multiple low mass planets in its habitable zone. They also considered a model with correlated noise (modified ARMA model described in Tuomi et al. 2013 and Sec. 5.1 of this paper) but found that white noise model is favoured by the data.

It has already been shown that noise in photometric observations of exoplanetary transits is often correlated (Pont et al. 2006). Information content of correlated data is lower than if the data were uncorrelated, therefore ignoring correlated noise components can result in spurious detection. In this paper, we present a Bayesian method for the analysis of RV data-sets with correlated noise. We also allow for the possibility of the reported uncertainty values on RV measurement to be over or under-estimated and deal with any inconsistencies between different data-sets in a statistically robust manner. We apply this method to the RV data-set of GJ667C.

The outline of this paper is as follows. We give a brief introduction to Bayesian inference in Sec. 2 and describe our object detection method for calculating the number of planets favoured by the data in Sec. 3. Our method for modelling RV data is described in Sec. 4. In Sec. 5 we describe our Bayesian analysis methodology

including the likelihood function and choice of prior distributions. We apply our method to RV data sets of GJ667C in Sec. 6 and present our conclusions in Sec. 7.

2 BAYESIAN INFERENCE

Bayesian inference provides a consistent approach to the estimation of a set of parameters Θ in a model (or hypothesis) H for the data D . Bayes’ theorem states that

$$\Pr(\Theta|D, H) = \frac{\Pr(D|\Theta, H) \Pr(\Theta|H)}{\Pr(D|H)}, \quad (1)$$

where $\Pr(\Theta|D, H) \equiv P(\Theta|D)$ is the posterior probability distribution of the parameters, $\Pr(D|\Theta, H) \equiv \mathcal{L}(\Theta)$ is the likelihood, $\Pr(\Theta|H) \equiv \pi(\Theta)$ is the prior, and $\Pr(D|H) \equiv \mathcal{Z}$ is the Bayesian evidence given by:

$$\mathcal{Z} = \int \mathcal{L}(\Theta)\pi(\Theta)d^N \Theta, \quad (2)$$

where N is the dimensionality of the parameter space. Bayesian evidence being independent of the parameters, can be ignored in parameter estimation problems and inferences can be obtained by taking samples from the (unnormalized) posterior distribution using standard MCMC methods.

Model selection between two competing models H_0 and H_1 can be done by comparing their respective posterior probabilities given the observed data-set D , as follows

$$R = \frac{\Pr(H_1|D)}{\Pr(H_0|D)} = \frac{\Pr(D|H_1) \Pr(H_1)}{\Pr(D|H_0) \Pr(H_0)} = \frac{\mathcal{Z}_1 \Pr(H_1)}{\mathcal{Z}_0 \Pr(H_0)}, \quad (3)$$

where $\Pr(H_1)/\Pr(H_0)$ is the prior probability ratio for the two models, which can often be set to unity in situations where there is not a prior reason for preferring one model over the other, but occasionally requires further consideration. It can be seen from (3) that the Bayesian evidence plays a central role in Bayesian model selection.

As the average of the likelihood over the prior, the evidence is larger for a model if more of its parameter space is likely and smaller for a model with large areas in its parameter space having low likelihood values, even if the likelihood function is very highly peaked. Thus, the evidence automatically implements Occam’s razor.

Evaluation of the multidimensional integral in (2) is a challenging numerical task. Standard techniques like thermodynamic integration are extremely computationally expensive which makes evidence evaluation at least an order of magnitude more costly than parameter estimation. Various alternative information criteria for astrophysical model selection are discussed by Liddle (2007), but the evidence remains the preferred method.

The nested sampling approach, introduced by Skilling (2004), is a Monte Carlo method targeted at the efficient calculation of the evidence, but also produces posterior inferences as a by-product. Feroz & Hobson (2008); Feroz et al. (2009, 2013) built on this nested sampling framework and have introduced the MULTINEST algorithm which is very efficient in sampling from posteriors that may contain multiple modes and/or large (curving) degeneracies and also calculates the evidence. This technique has greatly reduces the computational cost of Bayesian parameter estimation and model selection and has already been applied to several inference problems in astro and particle physics (see e.g. Feroz et al. 2008, 2009; Bridges et al. 2009; Feroz et al. 2009; Bridges et al. 2011; Strege et al. 2013; Karpenka et al. 2013).

3 BAYESIAN OBJECT DETECTION

To detect and characterise an unknown number of objects in a data-set, one would ideally like to infer simultaneously the full set of parameters $\Theta = \{N_{\text{obj}}, \Theta_1, \Theta_2, \dots, \Theta_{N_{\text{obj}}}, \Theta_n\}$, where N_{obj} is the (unknown) number of objects, Θ_i are the parameters values associated with the i th object, and Θ_n is the set of (nuisance) parameters common to all the objects. This, however, requires any sampling based approach to move between spaces of different dimensionality as the length of the parameter vector depends on the unknown value of N_{obj} . Such techniques are discussed in Hobson & McLachlan (2003) and Brewer et al. (2013). Nevertheless, due to this additional complexity of variable dimensionality, these techniques are generally extremely computationally intensive.

An alternative approach for achieving virtually the same result is the ‘multiple source model’. By considering a *series* of models $H_{N_{\text{obj}}}$, each with a *fixed* number of objects, i.e. with $N_{\text{obj}} = 0, 1, 2, \dots$. One then infers N_{obs} by identifying the model with the largest marginal posterior probability $\Pr(H_{N_{\text{obj}}}|\mathbf{D})$. Assuming that there are n_p parameters per object and n_n (nuisance) parameters common to all the objects, for N_{obj} objects, there would be $N_{\text{obj}}n_p + n_n$ parameters to be inferred. Along with this increase in dimensionality, the complexity of the problem also increases with N_{obj} due to the exponential increase in the number of modes as a result of counting degeneracy (there are $n!$ more modes for $N_{\text{obj}} = n$ than for $N_{\text{obj}} = 1$).

If the contributions to the data from each object are reasonably well separated and the correlations between parameters across objects is minimal, one can use the alternative approach of ‘single source model’ by setting $N_{\text{obj}} = 1$ and therefore the model for the data consists of only a single object. This does not, however, restrict us to detecting only one object in the data. By modelling the data in such a way, we would expect the posterior distribution to possess numerous peaks, each corresponding to the location of one of the objects. Consequently the high dimensionality of the problem is traded with high multi-modality in this approach, which, depending on the statistical method employed for exploring the parameter space, could potentially simplify the problem enormously. For an application of this approach in detecting galaxy cluster from weak lensing data-sets see Feroz et al. (2008).

Calculating Bayesian evidence accurately for large number of objects is extremely difficult, due to the increase in dimensionality and severe complexity of the posterior, but parameter estimation can still be done accurately. In order to circumvent this problem, Feroz et al. (2011) proposed a new general approach to Bayesian object detection called the ‘residual data model’ that is applicable even for systems with a large number of planets. This method is based on the analysis of residual data after detection of N_{obj} objects. We summarize this method below.

Let $H_{N_{\text{obj}}}$ denote a model with N_{obj} objects. The observed (fixed) data is denoted by $\mathbf{D} = \{d_1, d_2, \dots, d_M\}$, with the associated uncertainties being $\{\sigma_1, \sigma_2, \dots, \sigma_M\}$. In the general case that $N_{\text{obj}} = n$, the random variable \mathbf{D}_n is defined as a realisation of the data that would be collected if the model H_n were correct, and the random variable $\mathbf{R}_n \equiv \mathbf{D} - \mathbf{D}_n$, as the corresponding data residuals in this case. If one analyses the observed data \mathbf{D} to obtain samples from the posterior distribution of the model parameters Θ , it is straightforward to obtain samples from the posterior distribution of the data residuals \mathbf{R}_n . This is given by

$$\Pr(\mathbf{R}_n|\mathbf{D}, H_n) = \int \Pr(\mathbf{R}_n|\Theta, H_n) \Pr(\Theta|\mathbf{D}, H_n) d\Theta, \quad (4)$$

where

$$\Pr(\mathbf{R}_n|\Theta, H_n) = \prod_{i=1}^M \frac{1}{\sqrt{2\pi\sigma_i^2}} \exp \left\{ -\frac{[D_i - R_i - D_{p,i}(\Theta)]^2}{2\sigma_i^2} \right\}, \quad (5)$$

and $D_p(\Theta)$ is the (noiseless) predicted data-set corresponding to the parameter values Θ . Assuming that the residuals are independently Gaussian distributed with mean $\langle \mathbf{R}_n \rangle = \{r_1, r_2, \dots, r_M\}$ and standard deviations $\{\sigma'_1, \sigma'_2, \dots, \sigma'_M\}$ obtained from the posterior samples, $\langle \mathbf{R}_n \rangle$ can then be analysed with $N_{\text{obj}} = 0$, giving the ‘residual null evidence’ $Z_{r,0}$, which is compared with the evidence value $Z_{r,1}$ obtained by analysing $\langle \mathbf{R}_n \rangle$ with $N_{\text{obj}} = 1$. The comparison is thus being made between the model H_0 that the residual data does not contain an additional object and the model H_1 in which an additional object is present.

With no prior information about the number of objects in a data-set, the original data-set \mathbf{D} is first analysed with $N_{\text{obj}} = 1$. If, in the analysis of the corresponding residuals data, H_1 is favoured over H_0 , then the original data \mathbf{D} are analysed with $N_{\text{obj}} = 2$ and the same process is repeated. In this way, N_{obj} is increased in the analysis of the original data \mathbf{D} , until H_0 is favoured over H_1 in the analysis of the corresponding residual data. The resulting value for N_{obj} gives the number of objects favoured by the data. This approach thus requires the detection and estimation of orbital parameters for $N_{\text{obj}} = n$ model but the Bayesian evidence needs to be calculated only for the $N_{\text{obj}} = 1$ model (and the $N_{\text{obj}} = 0$ model, which is trivial); this reduces the computational cost of the problem significantly. We use this method for analysing the RV data-sets in this paper.

4 MODELLING RADIAL VELOCITIES

Observing planets at interstellar distances directly is extremely difficult, since the planets only reflect the light incident on them from their host star and are consequently many times fainter. Nonetheless, the gravitational force between the planets and their host star results in the planets and star revolving around their common centre of mass. This produces doppler shifts in the spectrum of the host star according to its RV, the velocity along the line-of-sight to the observer. Several such measurements, usually over an extended period of time, can then be used to detect extrasolar planets.

Following the formalism given in Balan & Lahav (2009), for N_p planets and ignoring the planet-planet interactions, the RV at an instant t_i observed at j th observatory can be calculated as:

$$v(t_i, j) = V_j - \sum_{p=1}^{N_p} K_p [\sin(f_{i,p} + \varpi_p) + e_p \sin(\varpi_p)], \quad (6)$$

where

- V_j = systematic velocity with reference to j th observatory,
- K_p = velocity semi-amplitude of the p th planet,
- ϖ_p = longitude of periastron of the p th planet,
- $f_{i,p}$ = true anomaly of the p th planet,
- e_p = orbital eccentricity of the p th planet,
start of data taking, at which periastron occurred.

Note that $f_{i,p}$ is itself a function of e_p , the orbital period P_p of the p th planet, and the fraction χ_p of an orbit of the p th planet, prior to the start of data taking, at which periastron occurred. While there is a unique mean line-of-sight velocity of the center of motion, it is

important to have a different velocity reference V_j for each observatory/spectrograph pair, since the velocities are measured differentially relative to a reference frame specific to each observatory.

Occasionally, there is a long-term linear drift in the RV data owing to the presence of a distant stellar companion. In such cases, one adds a corresponding linear drift term to (6) as follows:

$$v(t_i, j) = V_j - \sum_{p=1}^{N_p} K_p [\sin(f_{i,p} + \varpi_p) + e_p \sin(\varpi_p)] + g(t_i - t_0), \quad (7)$$

where g is the drift acceleration and t_0 is the time of first RV observation.

The measurement uncertainties on the RV data are assumed to be uncorrelated and Gaussian-distributed. In order to allow, however, for the possibility that the quoted measurement uncertainties are over- or under-estimated, we introduce a hyper-parameter α_j , for each observatory. The uncertainty on i th RV measurement from j th observatory, $\sigma_{i,j}$ is modified to become $\sigma_{i,j}/\alpha_j$. As discussed in Hobson, Bridle & Lahav (2002), these hyper-parameters effectively assign a weight to each data-set that is determined directly by its own statistical properties, and which are then marginalized over. This approach allows for the consistent statistical analysis of multiple data-sets even when they would otherwise be mutually inconsistent assuming the quoted measurement uncertainties. This contrasts sharply with the common subjective practice of simply excluding certain data-sets altogether, thereby assigning them a weight of zero.

In order to model the possible presence of an additional correlated noise component between RVs, which also simultaneously allows us to model intrinsic stellar variability ('jitter'), we adopt the red noise model of Baluev (2011, 2013). This approach is equivalent to assuming the presence of an additional term $s(t_i, j)$ on the right-hand side of (6) or (7) that has a covariance function given by

$$R[s(t_i, j), s(t_{i'}, j')] = s_j^2 \delta_{jj'} \exp(-|t_i - t_{i'}|/\tau_j), \quad (8)$$

where $\delta_{jj'}$ is the Kronecker delta symbol and τ_j is an unknown parameter characterising the correlation timescale for the j th observatory. For large enough τ_j , (8) becomes:

$$R[s(t_i, j), s(t_{i'}, j')] = s_j^2 \delta_{jj'} \delta_{ii'}, \quad (9)$$

which is the often used 'jitter' noise model with no correlated component. It is worth noting, however, that the correlated noise component modelled by (8) is generic and need not arise from intrinsic stellar variability. Indeed, the standard white noise model should be considered as nested within the red noise model used in this work.

Therefore, in our model for the RV data, we have five free parameters K , ϖ , e , P and χ for each planet, and an additional linear drift acceleration parameter g when there is linear drift in the data, common to all the planets. In addition to these parameters there are four nuisance parameters V_j , s_j , α_j and τ_j per observatory. The orbital parameters can be used along with the stellar mass m_s to calculate the length a of the semi-major axis of the planet's orbit around the centre of mass and the planetary mass m as follows:

$$a_s \sin i = \frac{KP\sqrt{1-e^2}}{2\pi}, \quad (10)$$

$$m \sin i \approx \frac{Km_s^{\frac{2}{3}}P^{\frac{1}{3}}\sqrt{1-e^2}}{(2\pi G)^{\frac{1}{3}}}, \quad (11)$$

$$a \approx \frac{m_s a_s \sin i}{m \sin i}, \quad (12)$$

where a_s is the semi-major axis of the stellar orbit about the centre-of-mass and i is the angle between the direction normal to the

planet's orbital plane and the observer's line of sight. Since i cannot be measured with RV data, only a lower bound on the planetary mass m can be estimated.

5 BAYESIAN ANALYSIS OF RADIAL VELOCITY MEASUREMENTS

There are several RV search programmes looking for extrasolar planets. The RV measurements consist of the time t_i of the i th observation, the measured RV v_i relative to a reference frame and the corresponding measurement uncertainty σ_i . These RV measurements can be analysed using Bayes' theorem given in (1) to obtain the posterior probability distributions of the model parameters discussed in the previous section. We now describe the form of the likelihood and prior probability distributions.

5.1 Likelihood function

As discussed in Gregory (2007), the errors on RV measurements can be treated as Gaussian and therefore the likelihood function can be written as

$$\mathcal{L}(\Theta) = \frac{1}{|2\pi\mathbf{C}|^{1/2}} \exp\left[-\frac{1}{2}(\mathbf{v} - \mathbf{v}')^t \mathbf{C}^{-1}(\mathbf{v} - \mathbf{v}')\right], \quad (13)$$

where \mathbf{v} is the vector with RV measurements $v(t_i, j)$, \mathbf{v}' is the vector with RVs $v(\Theta; t_i, j)$ calculated using (7), and \mathbf{C} is the covariance matrix. As discussed above, our model for the RV data includes hyper-parameters that scale the independent measurement uncertainties for each observatory and a correlated red noise component in (8), such that the total covariance function is given by

$$\mathcal{C}[v(t_i, j), v(t_{i'}, j')] = [(\sigma_{i,j}/\alpha_j)^2 \delta_{ii'} + s_j^2 \exp(-|t_i - t_{i'}|/\tau_j)] \delta_{jj'}. \quad (14)$$

This should be contrasted with the common practice when analysing RV data-sets of adopting a 'white' noise model using the quoted measurement uncertainties directly and ignoring any correlated noise component, but still including a stellar jitter term, in which case the covariance function is simply

$$\mathcal{C}_{\text{white}}[v(t_i, j), v(t_{i'}, j')] = (\sigma_{i,j}^2 + s_j^2) \delta_{ii'} \delta_{jj'}. \quad (15)$$

It should be noted that the red noise model used in this work differs markedly from the so-called 'ARMA' (autoregressive moving-average) model used in Tuomi et al. (2013) for modelling the correlated noise component. The AR part of the ARMA model, with order p models a time series X_i as follows:

$$X_i = c + \sum_{i'=1}^p \psi_{i'} X_{i-i'} + \epsilon_i, \quad (16)$$

where $\psi_{i'}$ are the AR coefficients, c is a constant and ϵ_i is the white noise term. AR(p) works well for regularly spaced time series but since the RV measurements are almost always irregularly spaced in time, this model in its original form is not applicable. In order to circumvent this problem, Tuomi et al. (2013) modified the AR model given in (16) as follows:

$$X_i = c + \sum_{i'=1}^p \psi_{i,i'} X_{i-i'} + \epsilon_i, \quad (17)$$

where

$$\psi_{i,i'} = \psi_{i'} \exp[\gamma(t_i - t_{i'})]. \quad (18)$$

Parameter	Prior	Mathematical Form	Lower Bound	Upper Bound
P (days)	Jeffreys	$\frac{1}{P \ln(P_{\max}/P_{\min})}$	0.2	365,000
K (m/s)	Mod. Jeffreys	$\frac{(K+K_0)^{-1}}{\ln(1+(K_{\max}/K_0)(P_{\min}/P_1)^{1/3}(1/\sqrt{1-e_1^2}))}$	0	$K_{\max}(P_{\min}/P_1)^{1/3}(1/\sqrt{1-e_1^2})$
V (m/s)	Uniform	$\frac{1}{V_{\min}-V_{\max}}$	$-K_{\max}$	K_{\max}
e	Uniform	1	0	1
ϖ (rad)	Uniform	$\frac{1}{2\pi}$	0	2π
χ	Uniform	1	0	1
s (m/s)	Mod. Jeffreys	$\frac{(s+s_0)^{-1}}{\ln(1+s_{\max}/s_0)}$	0	K_{\max}
α	Exponential	$e^{-\alpha}$	0	∞
τ (days)	Uniform	1	0	100

Table 1. Prior probability distributions.

One potential problem with this approach is that the sampling of time series at different points in time or at different time resolutions can have quite a large impact on the way the correlated noise component is modelled, as the $AR(p)$ part for calculating X_i includes the previous p time series values closest to X_i , regardless of their actual temporal separations. The red noise model that we have adopted correlates every single pair of RV measurements taken by a given observatory (with the magnitude of correlation dependent on the temporal separation within the pair) and therefore does not suffer from this shortcoming.

5.2 Choice of priors

For parameter estimation, priors become largely irrelevant once the data are sufficiently constraining, but for model selection the prior dependence always remains. Therefore, it is important that priors are selected based on physical considerations. We follow the choice of priors given in Gregory (2007), as shown in Table 1.

The modified Jeffreys prior,

$$\Pr(\theta|H) = \frac{1}{(\theta + \theta_0) \ln(1 + \theta_{\max}/\theta_0)}, \quad (19)$$

behaves like a uniform prior for $\theta \ll \theta_0$ and like a Jeffreys prior (uniform in log) for $\theta \gg \theta_0$. We set $K_0 = s_0 = 1$ m/s and $K_{\max} = 2129$ m/s, which corresponds to a maximum planet-star mass ratio of 0.01.

The prior distribution imposed on hyper-parameters α is exponential with expectation value unity. This is because our expectation is that the uncertainty values on observed RVs are neither over nor under-estimated, i.e. $E[\alpha] = 1$. With this constraint, and the fact that each α is a positive quantity, the correct prior distribution according to the maximum-entropy principle is the exponential prior (see e.g. Hobson et al. 2002; Sivia & Skilling 2006). When analysing multiple data-sets jointly, inferred values of hyper-parameters which are significantly away from unity, may hint at inconsistency between the data-sets. Nonetheless, inclusion of these hyper-parameters ensures a statistically consistent analysis of multiple data-sets even in this case (see Hobson et al. 2002 for more details).

6 RESULTS

We used the 172 RV measurements of GJ667C obtained by the HARPS spectrograph with the HARPS-TERRA technique,

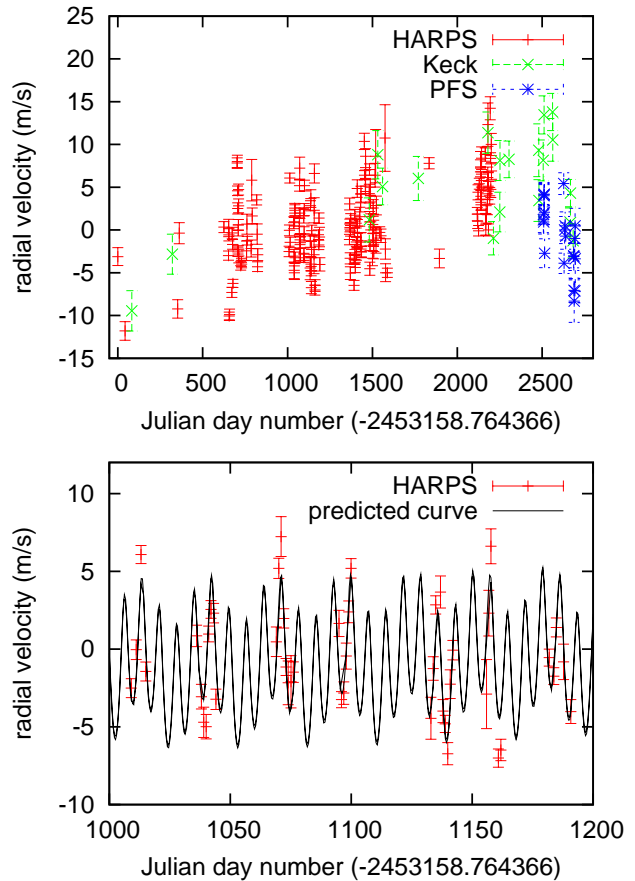


Figure 1. Top panel shows the radial velocity measurements for GJ667C from \mathcal{D}_{CCF} data-set, with the quoted 1σ errorbars. Bottom panel shows a blow-up of the mean fitted radial velocity curve to the data for two planets found orbiting GJ667C, with the red noise component included in the analysis.

20 measurements obtained with HIRES/Keck and 32 measurements with PFS/Megellan, we call this data-set \mathcal{D}_{TERRA} . We also analysed a separate data-set called \mathcal{D}_{CCF} , containing 170 RV measurements obtained by HARPS with the CCF technique, along with the same RV measurements from HIRES/Keck and PFS/Megellan. Both TERRA and CCF HARPS RV measurements are given in Anglada-Escude et al. (2013), while

N_p	\mathcal{D}_{CCF}		$\mathcal{D}_{\text{TERRA}}$	
	white noise	red noise	white noise	red noise
1	17.05 ± 0.16	4.22 ± 0.16	16.95 ± 0.16	6.82 ± 0.16
2	9.80 ± 0.16	2.24 ± 0.15	18.94 ± 0.16	5.00 ± 0.16
3	2.57 ± 0.15	0.44 ± 0.14	4.22 ± 0.15	0.89 ± 0.15
4	0.13 ± 0.14	0.16 ± 0.14	1.37 ± 0.15	0.00 ± 0.15
5			-0.49 ± 0.14	

Table 2. $\Delta \ln \mathcal{Z}_r$ values for the system GJ667C.

HIRES/Keck and PFS/Megellan RV measurements are available from Anglada-Escude & Butler (2012). Throughout this work, we ignore the planet-planet interactions and calculate the RVs by assuming Keplerian orbits for the planets.

The RVs from \mathcal{D}_{CCF} along with their $1 - \sigma$ uncertainty values are plotted in the top panel of Fig. 1. There is an evident long-term linear drift in RVs of GJ667C induced by its companion stellar pair GJ667AB, with expected value $\sim 3 \text{ m s}^{-1} \text{ yr}^{-1}$ (for a total mass of GJ667AB of $1.27 M_{\odot}$ and separation between GJ667AB and GJ667C of $\sim 300 \text{ AU}$) (Delfosse et al. 2013). We therefore added an additional drift component to RVs calculated, as given in (7). There is some hint of correlation between nearby values but due to irregular temporal sampling, it is difficult to discern any pattern by visual inspection.

We first address the question of whether there is evidence for the presence of correlated noise in the RV data-set of GJ667C. By comparing the evidence values for models with white and red noise, one could attempt to answer the question whether this system favours correlated red noise model over uncorrelated white noise. For the \mathcal{D}_{CCF} ($\mathcal{D}_{\text{TERRA}}$) data-set, $\Delta \ln \mathcal{Z}$ in favour of red noise for $N_p = 0$ and $N_p = 1$ is found to be 18.50 ± 0.37 (19.77 ± 0.37) and 35.83 ± 0.34 (45.46 ± 0.35) respectively, clearly showing very strong evidence in favour of the correlated noise model. Another way to distinguish between these two noise models would be to determine whether very large values of correlation timescale τ are ruled out when the red noise component is included in the analysis. Looking ahead, the 1-D marginalised posterior probability distributions for correlation timescales τ_H , τ_K and τ_P of HARPS, Keck and PFS, for $N_p = 2$ planets in the analysis of data-set \mathcal{D}_{CCF} are shown in Fig. 6. It is clear from these plots that there is a reasonably tight constraint on τ_H around ~ 9 days while the posteriors for τ_K and τ_P are largely unconstrained. Posterior distributions of τ from the analysis of data-set $\mathcal{D}_{\text{TERRA}}$ are similar. We can therefore be confident that the HARPS data strongly favours correlated red noise model over the uncorrelated white noise model. The Keck and PFS data-sets are not sufficiently discriminative, largely due to not having enough data points, to rule out either the white or the red noise model.

The origin of this correlated red noise is not entirely clear. It has already been shown that noise in photometric observations of exoplanetary transits is often correlated (Pont et al. 2006). Furthermore, O’Toole et al. (2008) showed that RV noise is not necessarily white due to stellar oscillations. Studies of couple of other M dwarves GJ876 and GJ581 have also found strong evidence for the presence of red noise (Baluev 2011, 2013). The correlation timescale of order 9 days found in this study, is too long to be explained by stellar oscillations alone and therefore could be due to a combination of several stellar effects.

In order to determine the number of planets supported by the RV data-sets of GJ667C, we follow the object detection method-

ology outlined in Sec. 3 and analyse the RV data, for both the correlated red noise and uncorrelated white noise models, starting with $N_p = 0$ and increasing it until the residual evidence ratio $\Delta \ln \mathcal{Z}_r \simeq 0$. These evidence ratios, obtained from the residuals after analysing the original data with a model containing N_p planets, are presented in Table 2. For each value of N_p , we also plot in Figs 2 and 3 the corresponding marginalised posterior probability distributions for the orbital period P obtained from the analysis of the residuals data, for data-sets \mathcal{D}_{CCF} and $\mathcal{D}_{\text{TERRA}}$ respectively. The combination of these residual posterior plots with the residual evidence values can be viewed as the Bayesian analogue of the Lomb–Scargle periodogram, with the residual evidences quantifying the level of confidence in the presence of any additional planets. We reiterate, however, that in our main object detection analysis, if $\Delta \ln \mathcal{Z}_r \gtrsim 0$ for $N_p = n$, we analyse the *original* (rather than residual) data with the $N_p = n + 1$ planet model.

For the red noise model, one sees from Table 2 that both \mathcal{D}_{CCF} and $\mathcal{D}_{\text{TERRA}}$ show strong evidence for the presence of no more than three planets. For both data-sets, the $N_p = 2$ model yields the planets GJ667Cb and c, with periods 7.19d and 28.13d respectively. For the $N_p = 3$ model, however, one finds that the third planet has a period of 106d for \mathcal{D}_{CCF} and 91d for data-set $\mathcal{D}_{\text{TERRA}}$. Indeed, this is consistent with the posterior distributions of orbital period from the analysis of residuals data after the detection of three planets; as shown in Figs 2 and 3 these distributions peak at 91d and 106d, respectively, for data-sets \mathcal{D}_{CCF} and $\mathcal{D}_{\text{TERRA}}$. For the $N_p = 4$ model, one finds that all four signals (with periods 7.19d, 28.13d, 91d and 106d) are detected in both (original) data-sets \mathcal{D}_{CCF} and $\mathcal{D}_{\text{TERRA}}$.

The presence of the 106d signal has already been debated quite extensively (see e.g. Delfosse et al. 2013), with several studies attributing it to stellar rotation, since it is very close to the rotation period of the star of 105d. Moreover, the full width at half-maximum (FWHM) of the CCF, and the Ca-II H+K S-index in the Mount Wilson system (S-index), which are used as indicators of stellar activity, both show a peak at 105d (Anglada-Escude et al. 2012). We also cannot be sure about the presence of 91d signal, as it was detected as the fourth planet in the analysis of \mathcal{D}_{CCF} and the residual evidence for $N_p = 3$ in this case was found to be ~ 0 . Furthermore, both FWHM of the CCF, and the S-index show a peak at 91d, although the 105d peak in these indicators is much more prominent than the 91d peak (Anglada-Escude et al. 2012). We are therefore confident in our conclusion that the current RV data-set provides strong evidence only for 2 planets in this system. However, the presence of a third signal with period 91d can not be ruled out, but the confirmation of its planetary origins will only be possible with more RV observations. Adopting the two-planet model with the red noise component included, the estimated parameter values obtained from the analysis of \mathcal{D}_{CCF} are listed in Table 3 while the 1-D marginalised posterior probability distributions are shown in Figs. 4-6. The mean RV curve for the two-planet model is overlaid on the RV measurements in Fig. 1. The posterior distributions obtained from the analysis of $\mathcal{D}_{\text{TERRA}}$ are very similar and therefore we do not re-produce them here.

Assuming the white noise model, one can see from Table 2 that there is evidence for the presence of at least 4 and perhaps 5 signals depending on whether the \mathcal{D}_{CCF} or $\mathcal{D}_{\text{TERRA}}$ data-set is used. Apart from the four signals with orbital periods 7.19d, 28.13d, 91d and 106d, there are additional signals with periods 39d, 60d, 180d and 350d, as can be seen in Figs. 2 and 3. Some of these signals have already been presented as detected planets in several studies (see e.g. Gregory 2012; Anglada-Escude et al. 2013).

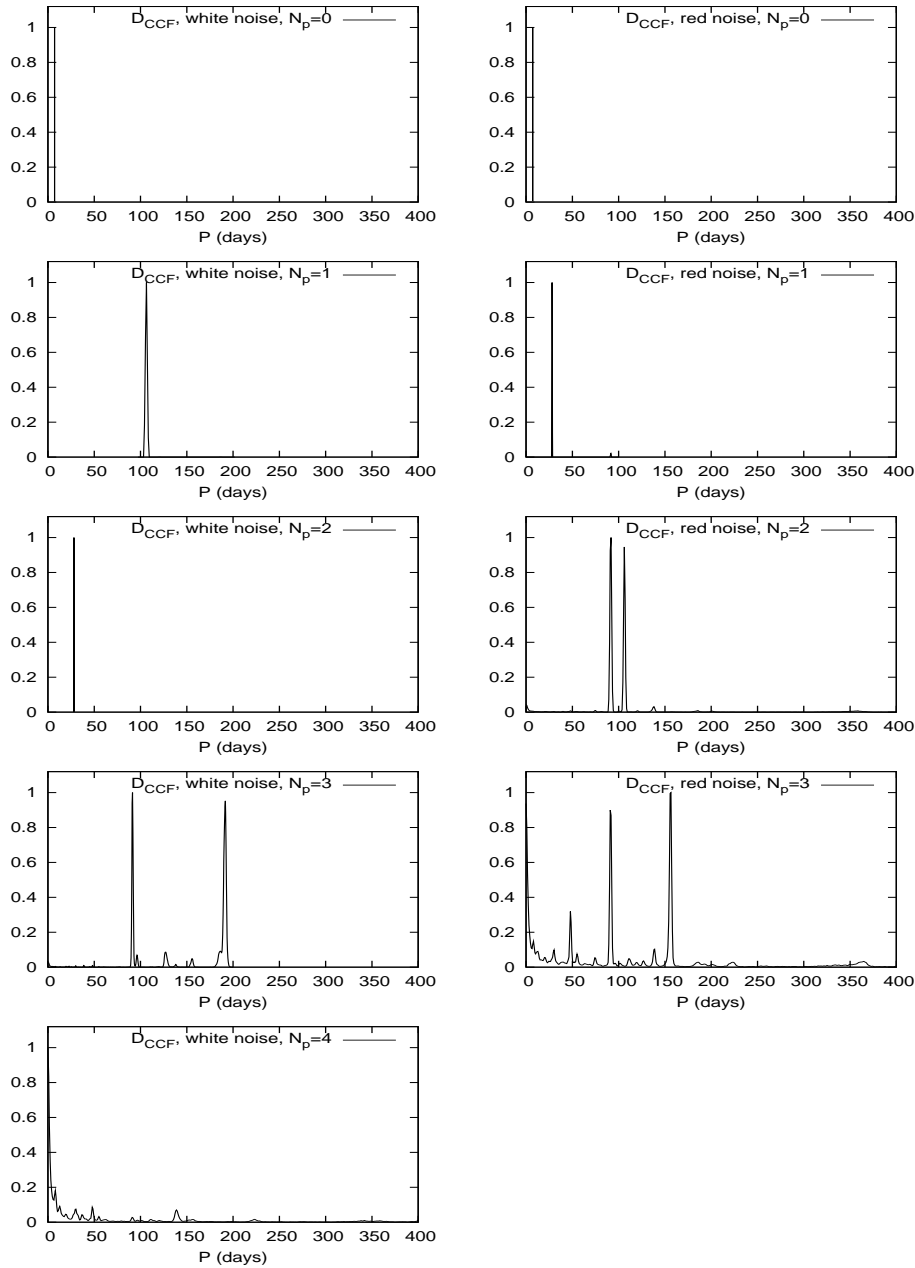


Figure 2. 1-D marginalised posterior probability distributions for the orbital period of planets found in the analysis of residual data calculated after the detection of N_p planets. Data-set \mathcal{D}_{CCF} was used in all cases.

Comparing the marginalised posterior probability distributions for the orbital period obtained from the analysis of residual data from white noise model (Figs. 2 and 3 left panel) to the red noise model (Figs. 2 and 3 right panel), we can see that there are quite a few more peaks in the white noise case, showing clear evidence that erroneously assuming the white noise model leads to spurious detections of planets. This also gives an explanation for the claims of detection of up to seven planets in this system.

Finally we note from Fig. 6 that the hyper-parameter α_H , allowing for any under or over-estimation of measurement uncertainty from the HARPS spectrograph is found to be 0.60 ± 0.06 (0.74 ± 0.08) in the analysis of \mathcal{D}_{CCF} (\mathcal{D}_{TERRA}) data-set, ruling out $\alpha = 1$ (no under or over-estimation in measurement uncertain-

ties) with high confidence. Therefore we conclude that the measured uncertainties from HARPS spectrograph for GJ667C have been under-estimated at the ~ 50 per cent level.

7 CONCLUSIONS

Detection of extrasolar planets using radial velocity (RV) observations requires the use of statistical model selection techniques. Most of these techniques assume the noise to be uncorrelated. Determining the number of planets from RV data-sets is already a very challenging task due to the problems associated with accurately calculating the probabilities for models with $N_p = 0, 1, 2, \dots$ plan-

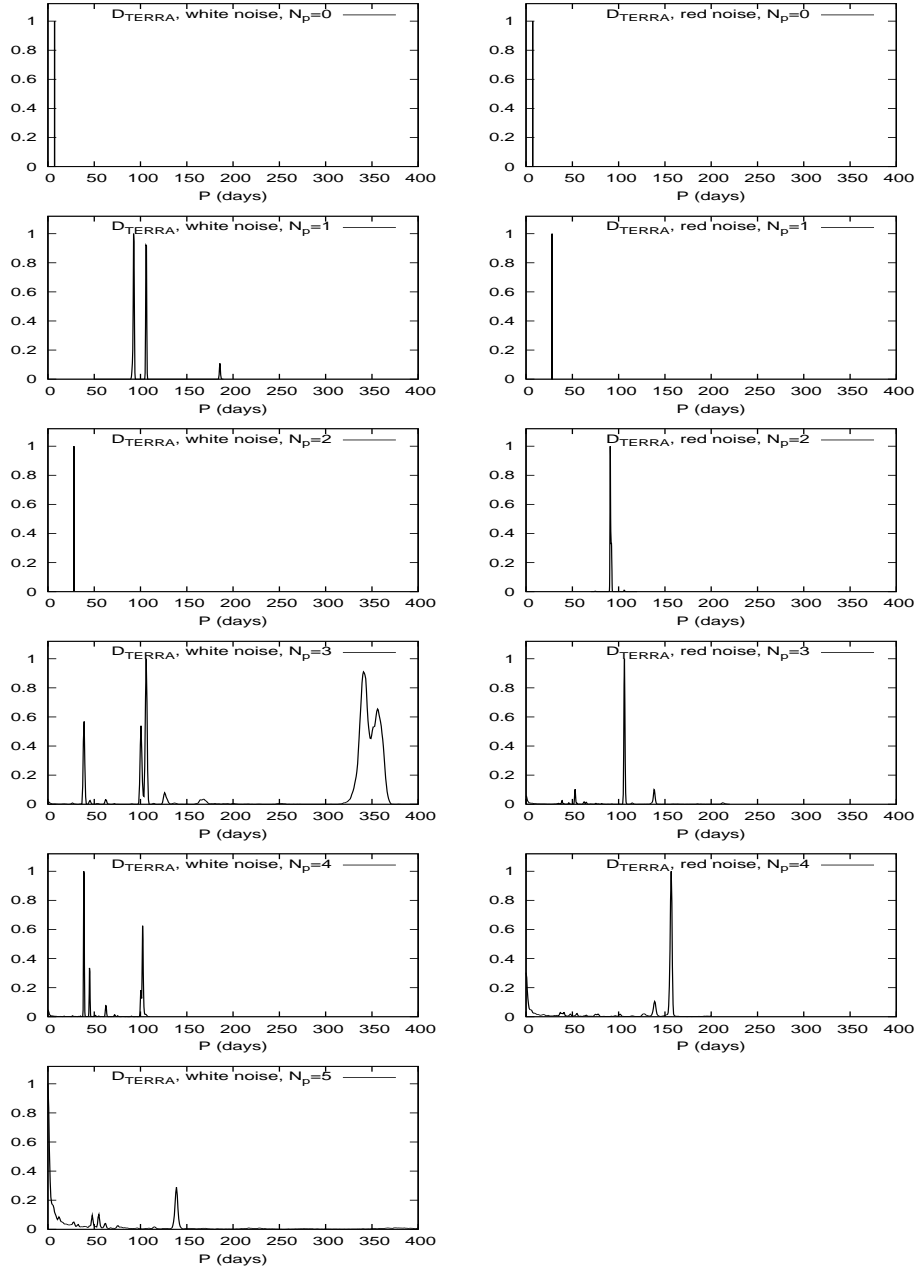


Figure 3. 1-D marginalised posterior probability distributions for the orbital period of planets found in the analysis of residual data calculated after the detection of N_p planets. Data-set $\mathcal{D}_{\text{TERRA}}$ was used in all cases.

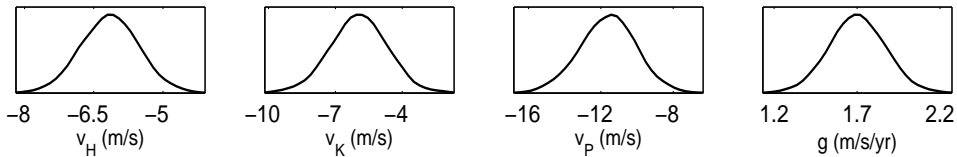


Figure 4. 1-D marginalised posterior probability distributions for the systematic velocities and drift acceleration of GJ667C system, obtained by assuming a two planet model, with red noise component included in analysis of data-set \mathcal{D}_{CCF} . Subscripts H, K and P refer to HARPS, Keck and PFS/Magellan spectrographs respectively.

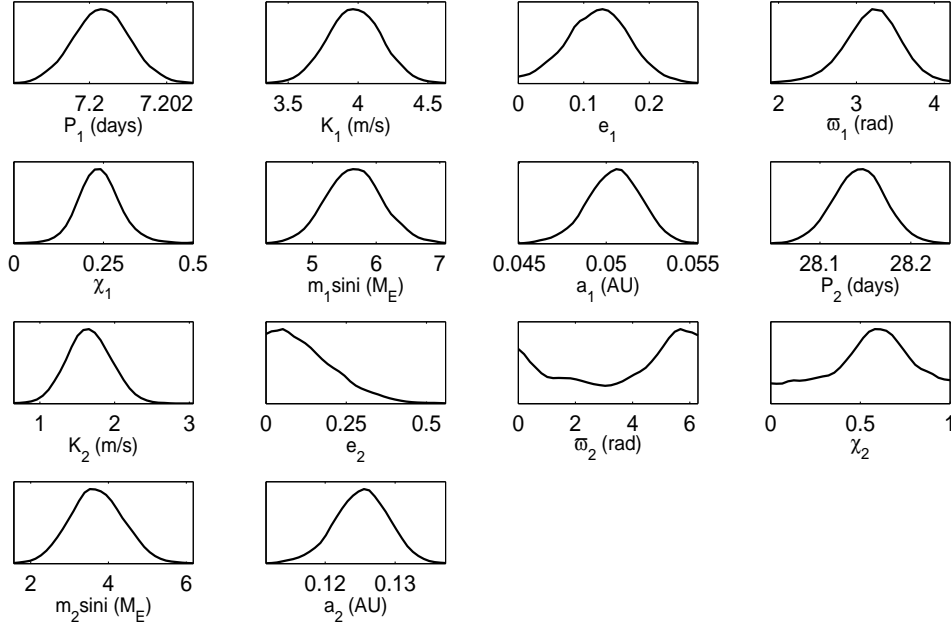


Figure 5. 1-D marginalised posterior probability distributions for the orbital parameters of the two planets, found orbiting GJ667C, in analysis of data-set \mathcal{D}_{CCF} , with the red noise component included.

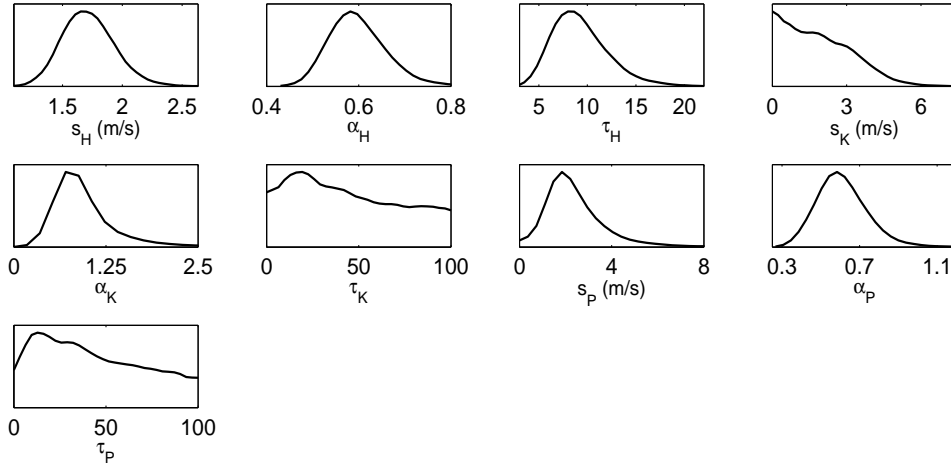


Figure 6. 1-D marginalised posterior probability distributions for the parameters specific to the noise model, with red noise component included, obtained by assuming a two planet model in analysis of data-set \mathcal{D}_{CCF} . Subscripts H, K and P refer to HARPS, Keck and PFS/Magellan spectrographs respectively.

ets. Allowing for correlated noise adds an additional layer of complexity to this problem. In this work, we have presented a Bayesian method for determining the number of planets supported by RV data-set in the presence of correlated red noise. The red noise model adopted collapses to a white noise model if correlated red noise is not supported by the data. Furthermore, we have introduced hyper-parameters allowing for any over or under-estimation of measurement uncertainties on RV observations. These hyper-parameters also allow us to deal with any inconsistencies between different data-sets in a statistically robust manner. In order to explore the parameter space of these models and perform Bayesian object detection, using the MULTINEST (Feroz & Hobson 2008; Feroz et al. 2009, 2013) algorithm whose accuracy has already been demonstrated in many diverse problems in astro and particle physics.

By applying this method to the RV data-set of GJ667C, we find conclusive evidence that the HARPS data favours correlated red noise model over uncorrelated white noise model with the correlation timescale ~ 9 days. Adopting the red noise model, we confirm the presence of planets GJ667Cb and c with periods 7.19d and 28.13d respectively. There is some evidence for a third signal with orbital period 91d, but the planetary origins of this signal are doubtful. We have also shown conclusively that erroneously adopting the white noise model can result in detection of multiple further planets, which also explains the recent claims of the detection of up to seven planets in this system. We also found strong evidence for the under-estimation of measurement uncertainties from the HARPS spectrograph for GJ667C at the ~ 50 per cent level which may hint towards some systematics in this data-set.

Parameter	GJ667Cb	GJ667Cc
P (days)	7.200 ± 0.001 (7.200)	28.143 ± 0.029 (28.126)
K (m/s)	3.977 ± 0.193 (4.116)	1.663 ± 0.291 (1.854)
e	0.122 ± 0.078 (0.121)	0.133 ± 0.098 (0.081)
ϖ (rad)	3.206 ± 0.395 (3.304)	3.659 ± 2.048 (0.443)
χ	0.241 ± 0.070 (0.222)	0.549 ± 0.236 (0.430)
$m \sin i$ (M_{\oplus})	5.661 ± 0.437 (5.826)	3.709 ± 0.682 (4.150)
a (AU)	0.050 ± 0.002 (0.050)	0.125 ± 0.004 (0.125)

Table 3. Estimated parameter values for the two planets found orbiting GJ667C, with the red noise component included in the analysis of dataset \mathcal{D}_{CCF} . The estimated values are quoted as $\mu \pm \sigma$ where μ and σ are the posterior mean and standard deviation respectively. The numbers in parenthesis are the maximum-likelihood parameter values.

The level of correlation found in the RV data-set of this system emphasizes the need to check robustly for such correlations before claiming detections of multi-planet systems. This is of vital importance as these multi-planet systems, especially those with planets inside the habitable zone, provide important data for research in many areas of planetary astrophysics.

Finally, we note that although the noise model adopted in this study does a far better job than a white noise model, it is still phenomenological and therefore it does not provide much information about the origin of correlated noise component. One would expect to improve the analysis even further by adopting physically motivated noise models.

ACKNOWLEDGEMENTS

This work was performed on COSMOS VIII, an SGI Altix UV1000 supercomputer, funded by SGI/Intel, HEPCE and PPARC, and the authors thank Andrey Kaliazin for assistance. The work also utilized the Darwin Supercomputer of the University of Cambridge High Performance Computing Service (<http://www.hpc.cam.ac.uk/>), provided by Dell Inc. using Strategic Research Infrastructure Funding from the Higher Education Funding Council for England. FF is supported by a Research Fellowship from the Leverhulme and Newton Trusts. We would also like to thank the anonymous referee for very useful comments.

REFERENCES

- Anglada-Escude G., Arriagada P., Vogt S. S., Rivera E. J., Butler R. P., Crane J. D., Shectman S. A., Thompson I. B., Minniti D., Haghhighipour N., Carter B. D., Tinney C. G., Wittenmyer R. A., Bailey J. A., O’Toole S. J., Jones H. R. A., Jenkins J. S., 2012, *ApJ*, 751, L16
- Anglada-Escude G., Butler R. P., 2012, *ApJS*, 200, 15
- Anglada-Escude G., Tuomi M., Gerlach E., Barnes R., Heller R., Jenkins J. S., Wende S., Vogt S. S., Butler R. P., Reiniers A., Jones H. R. A., 2013, arXiv e-prints [arXiv:1306.6074]
- Balan S. T., Lahav O., 2009, *MNRAS*, 394, 1936
- Baluev R. V., 2011, *Celestial Mechanics and Dynamical Astronomy*, 111, 235
- Baluev R. V., 2013, *MNRAS*, 429, 2052
- Bonfils X., Delfosse X., Udry S., Forveille T., Mayor M., Perrier C., Bouchy F., Gillon M., Lovis C., Pepe F., Queloz D., Santos N. C., Ségransan D., Bertaux J.-L., 2011, arXiv e-prints [arXiv:1111.5019]
- Brewer B. J., Foreman-Mackey D., Hogg D. W., 2013, *AJ*, 146, 7
- Bridges M., Cranmer K., Feroz F., Hobson M., Ruiz de Austri R., Trotta R., 2011, *Journal of High Energy Physics*, 3, 12
- Bridges M., Feroz F., Hobson M. P., Lasenby A. N., 2009, *MNRAS*, 400, 1075
- Delfosse X., Bonfils X., Forveille T., Udry S., Mayor M., Bouchy F., Gillon M., Lovis C., Neves V., Pepe F., Perrier C., Queloz D., Santos N. C., Ségransan D., 2013, *A&A*, 553, A8
- Feroz F., Balan S. T., Hobson M. P., 2011, *Monthly Notices of the Royal Astronomical Society*, 415, 3462
- Feroz F., Gair J. R., Hobson M. P., Porter E. K., 2009, *Classical and Quantum Gravity*, 26, 215003
- Feroz F., Hobson M. P., 2008, *MNRAS*, 384, 449
- Feroz F., Hobson M. P., Bridges M., 2009, *MNRAS*, 398, 1601
- Feroz F., Hobson M. P., Cameron E., Pettitt A. N., 2013, arXiv e-prints [arXiv:1306.2144]
- Feroz F., Hobson M. P., Zwart J. T. L., Saunders R. D. E., Grainge K. J. B., 2009, *MNRAS*, 398, 2049
- Feroz F., Marshall P. J., Hobson M. P., 2008, arXiv e-prints [arXiv:0810.0781]
- Ford E. B., 2005, *AJ*, 129, 1706
- Ford E. B., Gregory P. C., 2007, in G. J. Babu & E. D. Feigelson ed., *Statistical Challenges in Modern Astronomy IV Vol. 371 of Astronomical Society of the Pacific Conference Series, Bayesian Model Selection and Extrasolar Planet Detection*. pp 189–+
- Gregory P. C., 2005, *ApJ*, 631, 1198
- Gregory P. C., 2007, *MNRAS*, 374, 1321
- Gregory P. C., 2012, arXiv e-prints [arXiv:1212.4058]
- Hobson M. P., Bridle S. L., Lahav O., 2002, *MNRAS*, 335, 377
- Hobson M. P., McLachlan C., 2003, *MNRAS*, 338, 765
- Karpenka N. V., March M. C., Feroz F., Hobson M. P., 2013, *MNRAS*
- Liddle A. R., 2007, *MNRAS*, 377, L74
- Lomb N. R., 1976, *Ap&SS*, 39, 447
- Mackay D. J. C., 2003, *Information Theory, Inference and Learning Algorithms*. Cambridge University Press, Cambridge, UK
- O’Toole S. J., Tinney C. G., Jones H. R. A., 2008, *MNRAS*, 386, 516
- Pont F., Zucker S., Queloz D., 2006, *MNRAS*, 373, 231
- Scargle J. D., 1982, *ApJ*, 263, 835
- Sivia D., Skilling J., 2006, *Data Analysis A Bayesian Tutorial*. Oxford University Press
- Skilling J., 2004, in Fischer R., Preuss R., Toussaint U. V., eds, *American Institute of Physics Conference Series Nested Sampling*. pp 395–405
- Söderhjelm S., 1999, *A&A*, 341, 121
- Strege C., Bertone G., Feroz F., Fornasa M., Ruiz de Austri R., Trotta R., 2013, *Journal of Cosmology and Astroparticle Physics*, 4, 13
- Tuomi M., Jones H. R. A., Jenkins J. S., Tinney C. G., Butler R. P., Vogt S. S., Barnes J. R., Wittenmyer R. A., O’Toole S., Horner J., Bailey J., Carter B. D., Wright D. J., Salter G. S., Pinfield D., 2013, *A&A*, 551, A79